

 Open access • Proceedings Article • DOI:10.2514/6.2006-2955

Free-jet Testing of a REST Scramjet at Off-Design Conditions — [Source link](#)

Michael K. Smart, Edward G. Ruf

Institutions: Langley Research Center

Published on: 01 Jan 2006

Topics: Scramjet, Combustor, Fuel injection and Mach number

Related papers:

- [Design of Three-Dimensional Hypersonic Inlets with Rectangular-to-Elliptical Shape Transition](#)
- [Experimental testing of a hypersonic inlet with rectangular-to-elliptical shape transition](#)
- [Mach 4 Performance of Hypersonic Inlet with Rectangular-to-Elliptical Shape Transition](#)
- [Computational Investigation of the Performance and Back-Pressure Limits of a Hypersonic Inlet](#)
- [Operating characteristics of the Langley Mach 7 Scramjet Test Facility](#)

Share this paper:    

View more about this paper here: <https://typeset.io/papers/free-jet-testing-of-a-rest-scramjet-at-off-design-conditions-45a7gdrky>

Free-jet Testing of a REST Scramjet at Off-Design Conditions

Michael K Smart* and Edward G. Ruf[#]

NASA Langley Research Center

Hampton Virginia, 23681

Scramjet flowpaths employing elliptical combustors have the potential to improve structural efficiency and performance relative to those using planar geometries. NASA Langley has developed a scramjet flowpath integrated into a lifting body vehicle, while transitioning from a rectangular capture area to both an elliptical throat and combustor. This Rectangular-to-Elliptical Shape Transition (REST) scramjet, has a design point of Mach 7.1, and is intended to operate with fixed-geometry between Mach 4.5 and 8.0. This paper describes initial free-jet testing of the heat-sink REST scramjet engine model at conditions simulating Mach 5.3 flight. Combustion of gaseous hydrogen fuel at equivalence ratios between 0.5 and 1.5 generated robust performance after ignition with a silane-hydrogen pilot. Facility-model interactions were experienced for fuel equivalence ratios above 1.1, yet despite this, the flowpath was not unstirred by fuel addition at the Mach 5.3 test condition. Combustion tests at reduced stagnation enthalpy indicated that the engine self-started following termination of the fuel injection. Engine data is presented for the largest fuel equivalence ratio tested without facility interaction. These results indicate that this class of three-dimensional scramjet engine operates successfully at off-design conditions.

Nomenclature

I	vitiated heater O ₂ replenishment factor, ratio of the actual mass flow rate of O ₂ to that required to replace that consumed
H	enthalpy
M	Mach number
MW	molecular weight
t	time
p	pressure
T	temperature
ϕ	fuel equivalence ratio
γ	ratio of specific heats

Subscripts

0	flight
1	wind tunnel freestream or inlet entrance
st	stagnation

*Research Scientist; presently Associate Professor, Division of Mechanical Engineering, University of Queensland. Senior member AIAA.

[#]Aerospace Engineer; Hypersonic Airbreathing Propulsion Branch, Mail Stop 168

I. Introduction

The high-speed propulsion community is interested in scramjets as a propulsion system for both hypersonic cruise vehicles and access-to-space. As scramjets do not operate efficiently below Mach 3-4, they must utilize a low speed propulsion system (either gas-turbine or rocket) up to approximately Mach 3-4, at which point they begin operation and accelerate to higher speeds. Current scramjet technologies, based predominantly on planar flowpath geometries, are either point design configurations¹ or have been demonstrated in flight over a small Mach number range. Hence the most pressing challenge for scramjet technology at the present time is expansion of the operational Mach number envelope.

Over the past several years NASA Langley Research Center has addressed this issue through the development of airframe-integrated scramjets with “rounded” or elliptical combustors. The motivations for the work were three-fold:

1. To take advantage of the inherent structural efficiency of rounded structures. This potentially enables reduced structural weight.
2. To take advantage of the reduced wetted area of elliptical cross-sections relative to rectangular shapes for the same cross-sectional or flow area. (Reduced wetted area lowers viscous drag and cooling requirements in the high dynamic pressure combustor environment.)
3. To remove the potentially detrimental fluid dynamic effects of corner flows in scramjet isolators and combustors. This may improve the back-pressure limits of the inlet/isolator, or alternatively, reduce isolator length requirements.

The combination of these features is expected to lead to a scramjet engine with high overall system performance. As this work has progressed it became clear that this engine class is able to operate over a large Mach number range with fixed-geometry, further enhancing its potential system level benefits. Figure 1 depicts a potential elliptical-combustor scramjet installation on a lifting-body vehicle.

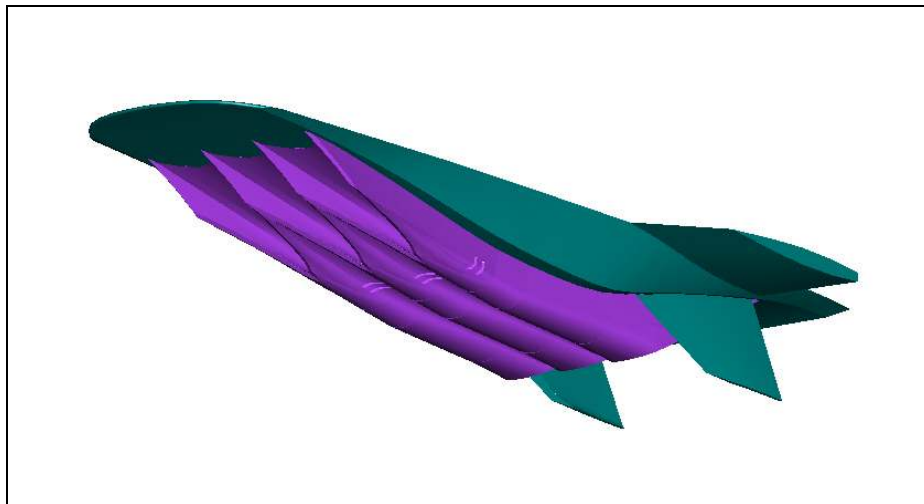


Figure 1. Hypersonic vehicle powered by REST Scramjet engine modules.

A key to airframe-integrated scramjets with elliptical combustors is the 3-D inlet shape transition. In particular, this is a transition from a rectangular-like capture area, dictated by modular installation of flowpaths on the vehicle, to an elliptical isolator/combustor shape. The design and testing of these Rectangular-to-Elliptical Shape Transition (REST) inlets, therefore, became a major research focus. The design

procedure developed for these inlets² utilized a quasi-streamline-tracing technique to produce an inlet with highly swept leading edges, a cut back cowl, and incorporate the required shape transition to end with an elliptical throat. The REST inlets resulting from these procedures have almost 100% mass capture at the design Mach number, and operate below the design Mach number by spilling air past the cut back cowl. An important aspect of the overall design procedure is the ability to minimize inlet length without violating shock wave/boundary layer separation criteria.



Figure 2. REST inlet model in the AHSTF.

Figure 2 shows a previous REST inlet model, with a design point of $M_1 = 6.0$, installed in the Arc Heated Scramjet Test Facility (AHSTF) at NASA Langley³. This inlet was designed to be installed on a vehicle with a short 6 degree forebody, hence the flight design point was $M_0 = 7.1$. Testing at $M_1 = 6.2$ showed that this inlet was highly efficient, and self-started with an internal contraction ratio well above the Kantrowitz limit³. However, this inlet would not start at $M_1 \sim 4.7$. Later, further testing was performed on several modified designs at $M_1 = 4.0$ to assess changes to the overall design procedure intended to extend the inlet operational regime to lower Mach numbers. These tests determined the performance, operability limits and self-starting characteristics of REST inlets well below the design point⁴. Together with a significant amount of CFD analysis⁵, these tests indicated that REST inlets are a viable fixed-geometry configuration for airframe-integrated scramjets in the Mach 4.5 to 8.0 flight regime.

After the operational range of this REST inlet design had been determined, research was re-focused on the design of the isolator/combustor configuration most appropriate for a REST scramjet operating between Mach 4.5 and 8.0. This work concentrated in two over-lapping areas; (1) the detailed design of injector geometries that were compatible with elliptical combustors, and (2) the determination of an isolator length and combustor area distribution that have the potential to produce desired performance levels over the range of conditions corresponding to Mach 4.5-8.0 flight. This work made significant use of both CFD and quasi-1-D cycle analysis. The results led to the design of an isolator/combustor configuration that incorporated a multiple-station injection system and a divergent elliptical combustor. The flowpath

design was completed with the addition of a nozzle that transitions back to a rectangular exit shape so as to integrate efficiently with a lifting body vehicle.

Verification that this class of scramjet is a viable configuration for hypersonic propulsion is best performed through free-jet testing of the complete flowpath. This paper describes results from a performance and operability verification test program that was undertaken in the Combustion Heated Scramjet Test Facility at NASA Langley. Tests were mainly performed at conditions simulating flight at Mach 5.3, though some testing was also performed at lower total enthalpy and pressure conditions. The overall research goal was to develop an understanding of the operational characteristics of this scramjet-class at conditions significantly below the design Mach number.

II. Wind Tunnel and Test Conditions

The experiments were performed in the NASA Langley Combustion Heated Scramjet Test Facility (CHSTF)^{6,7}. This wind-tunnel has a 96 in. long test chamber with a height of 42 in. and a width of 30 in., and was designed specifically for free-jet testing of complete scramjet flowpaths. This test program utilized the Mach 4.7 facility nozzle, which has a square exit with dimensions of 0.337m x 0.337m (13.26in x 13.26in.) With this nozzle in place, this facility simulates flight conditions between Mach 4.7 and 6.0 through the use of a hydrogen-air heater with oxygen replenishment. The primary contaminant in the test gas is water vapor. The exhaust from the test section is ducted to a 70 ft diameter vacuum sphere, and typical tests are between 10 and 30 seconds duration.

The tests described in this article were conducted at a total enthalpy equivalent to flight at Mach 5.3 and a total pressure corresponding to flight at a dynamic pressure of 47.7 kPa (1000 psf). For these conditions the Mach 4.7 nozzle approximately simulates the presence of a six-degree planar forebody compression. A survey of the nozzle exit flow was performed as part of this test program. This survey covered an 11in. wide by 8 in. high area in the center of the nozzle exit area. Figure 3 shows the Mach number contours calculated from the survey measurements, with an approximate outline of the engine capture stream tube shown. Table 1 lists the Mach 5.3 test conditions. Water vapor content of the test media at this condition is approximately 17.5 % on a molar basis.

Property	Test Point
p_{st} Mpa (psia)	2.068 (300)
T_{st} K (°R)	1230 (2215)
M_1	4.46
MW	27.618
γ	1.389

Table 1. Wind tunnel stagnation conditions and 1-D Mach number.

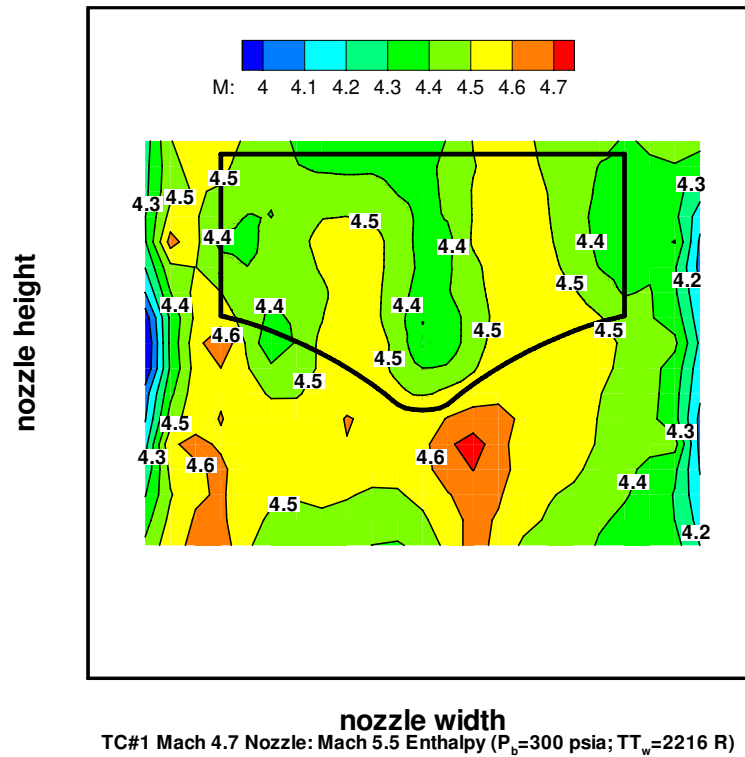


Figure 3. Mach number contours at the Mach 4.7 nozzle exit.



Figure 4. REST scramjet test article.

III. Engine Model and Instrumentation

Figure 4 shows the fully assembled engine model prior to installation in the wind tunnel. The test article, approximately 80 in. long by 8 in. wide, is of thick-walled copper construction for heat sink capability with, a maximum test duration of 30 seconds. As already indicated, the flowpath had a design point of Mach 7.1, and an intended operational range between Mach 4.5 and 8.0.

The engine model was comprised of four major components. First, the REST inlet, which was manufactured using an electro-forming technique to a maximum wall thickness of 0.4 in., with 0.030 in. leading edge radii. A truncated forebody plate 5 in. long and 9 in. wide was installed upstream of the inlet. Second, an elliptical injector block, which was constructed of copper and had all of the internal surfaces coated with a 0.015 in. layer of zirconia oxide for thermal protection. Third, a divergent elliptical combustor, which was constructed of copper with a wall thickness of 0.75 in., and which also had all internal surfaces coated with a 0.015 in. layer of zirconia. Fourth, a nozzle, which was manufactured in 2 sections: (i) a fully enclosed internal nozzle and, (ii) an asymmetric external nozzle. Both nozzle sections were constructed of copper, and transitioned back to a rectangular shape for efficient vehicle integration. These four components were assembled end-to-end, and attached to a steel backing plate in a manner which allowed the engine to freely expand longitudinally, and the entire engine assembly was suspended in the facility test section on a 6-component force balance.

The engine model was instrumented with 180 surface static pressure taps and 12 co-axial surface thermocouples. Pressure taps were distributed along nominal streamlines (at the on-design Mach number) on the internal surface of the inlet, with one external pressure tap at the inlet notch. The remaining engine internal pressure taps were situated on the body-side center-line, the cowl-side center-line, and lines along the left and right sides. Two co-axial thermocouples were situated in the inlet, nine were situated in the combustor, and one in the nozzle. The co-axial thermocouples in the combustor were coated with a layer of zirconia. The model surface static pressures were measured using a Pressure Systems Inc. Model 8400 electronically scanning pressure system. Four pressure ranges were utilized in the tests: 0-34.4 kPa (0-5 psia), 0-102.1 kPa (0-15 psia), 0-309.2 kPa (0-45 psia) and 0-680.7 kPa (0-100 psia). The error associated with the use of these transducers is +/- 0.5% of full scale. The type T co-axial surface thermocouples were manufactured by Medtherm Corporation and were electrically isolated from the model. The thermocouple output was converted to temperature by a universal temperature reference system and processed by a 16-bit NEFF A/D converter. The error associated with the use of these thermocouples was +/- 0.5% of the temperature measured above the 273 K reference. Additionally facility and fuel system data was also processed by the NEFF A/D converter. All data was recorded using the Autonet Version 4.0 data acquisition software on a personal computer and was recorded at a rate of 10 Hz.

Figure 5 shows the REST Scramjet installed in the CHSTF test section with the side-wall of the test section and facility diffuser removed. The tunnel flow is from right-to-left, and the engine model, wind-tunnel nozzle, force balance and fuel supply lines are labeled. All instrumentation was shielded from the high enthalpy flow for protection, as well as providing a streamlined external shape. The engine was fueled with room temperature gaseous hydrogen, and a gaseous 20% silane – 80% hydrogen (molar basis), pyrophoric pilot was used to promote fuel ignition.

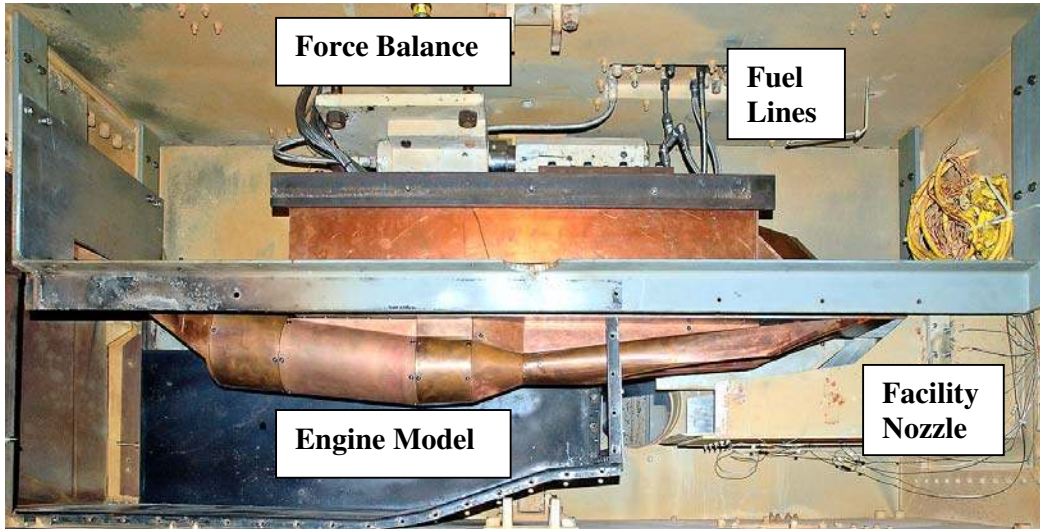


Figure 5. REST scramjet in the CHSTF.

IV. Experimental Results

The goals of the test program were two-fold: (1) to quantify the REST inlet performance and operability characteristics when incorporated within a complete engine flowpath; and (2) determine, for the first time, the overall performance attributes of this class of scramjet. A total of 45 engine tests were conducted, with the majority of the tests conducted at conditions simulating Mach 5.3 flight, at a dynamic pressure of 47.7kPa (1000 psf). A reduced number of tests were conducted at reduced stagnation enthalpy and/or pressure to investigate engine operability. The flowpath started with the facility for all tests. Fueled tests conducted at substantially lower stagnation enthalpy resulted in the engine unstarting. However, the engine self-started after the fuel injection was terminated.

No-fuel runs

Figure 6 shows the time histories of the facility stagnation conditions (p_{st} and T_{st}) and I for a typical run in the test program. The valve supplying hydrogen to the heater was opened at approximately $t = -1$ second, with a corresponding rise in the heater stagnation pressure and temperature. Time $t = 0$ seconds corresponded to the commanded opening of the oxygen replenishment valve. Steady-state conditions were established at approximately $t = 4$ seconds and continued in this run until $t = 13.5$ seconds, when the heater hydrogen and oxygen valves were closed and the test ended.

Figure 7 shows typical body-side and cowl-side pressure distributions on the internal surfaces of the flowpath with no-fuel addition. These pressure distributions indicated that the flowpath was started, as they exhibited a smooth increase in pressure on the body-side leading up to the inlet throat, shock dominated supersonic flow in the combustor, and decreasing pressure along the nozzle. The average of the eight circumferential pressure taps around the inlet just upstream of the throat indicated that the inlet pressure ratio was consistent with pre-test CFD predictions.

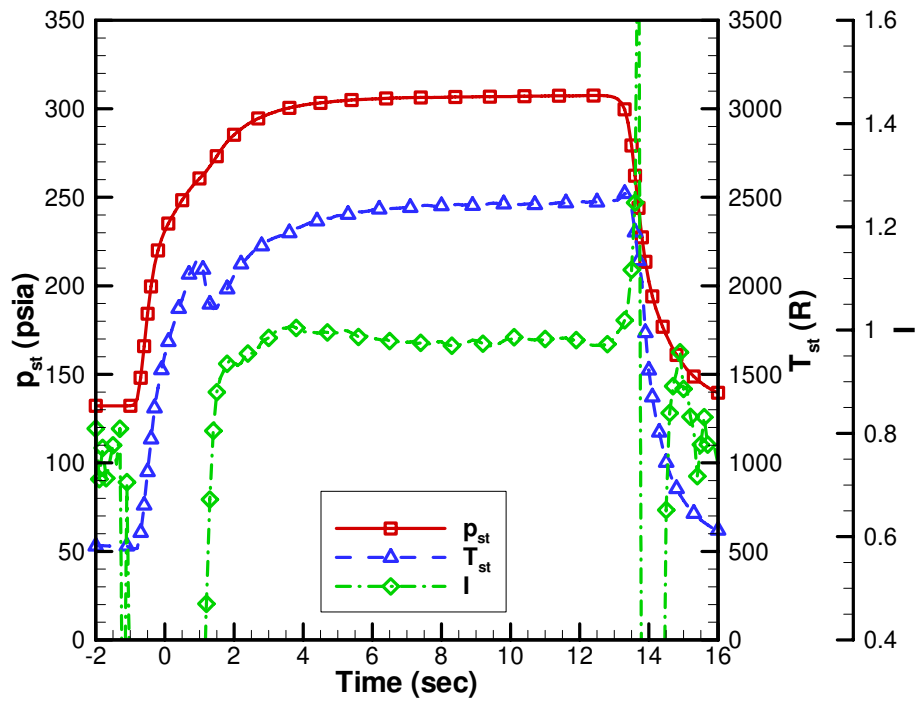


Figure 6. Time histories of facility stagnation conditions.

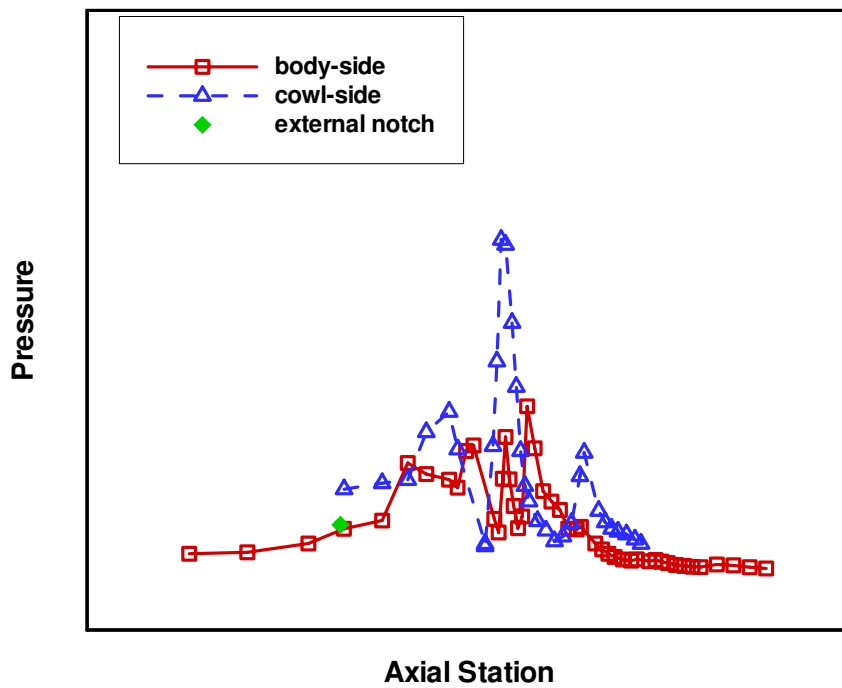


Figure 7. Flowpath pressure distributions with no fuel injection.

Fueled runs

Engine data is presented for a test corresponding to the maximum fuel injection flowrate without facility-model interaction. Figure 8 shows time histories of the drag force measured by the force balance and the fuel line pressure during a typical fueled run. At $t = 4.0$ seconds the drag force reached an approximately steady state value that corresponded to a started flowpath with no fuel injection. At approximately $t = 7.0$ seconds the silane-hydrogen pilot was turned on, initiating fuel flow to the engine and producing a corresponding reduction in the drag force. At approximately $t = 8.0$ seconds the pilot flow was reduced to zero and the hydrogen flow was increased to its steady state value for the test, corresponding to $\phi = 1.09$. This produced a further reduction in the drag force to a level consistent with robust combustion within the engine. At approximately $t = 10$ seconds the hydrogen fuel valve was closed and the facility heater propellant valves were closed at $t = 13.5$ seconds.

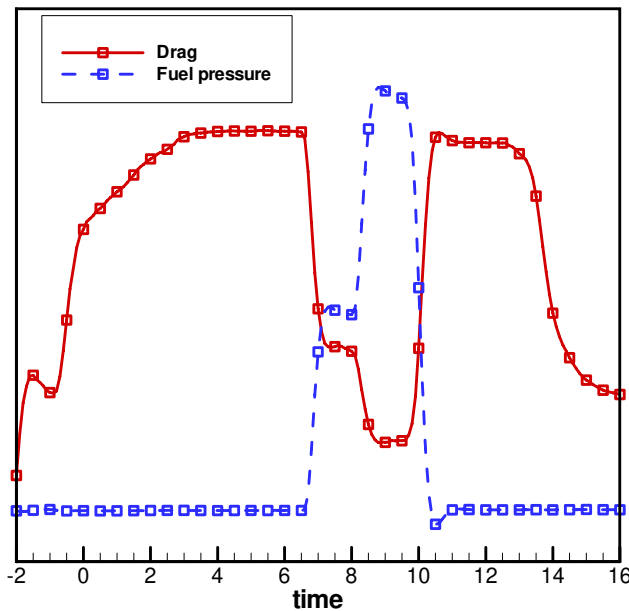


Figure 8. Time histories of drag force and fuel line pressure.

Figures 9 and 10 show the measured body-side and cowl-side pressure distributions, respectively, at different times during the test: $t = 6.5$ seconds (started flowpath with no-fuel), $t = 7.8$ seconds (silane-hydrogen pilot with $\phi = 0.59$) and $t = 9.8$ seconds (hydrogen fuel at $\phi = 1.09$). The pressure distribution at $t = 7.8$ seconds shows that the silane-hydrogen pilot significantly raised the pressure in the combustor, compared with no-fuel, and pushed the pre-combustion pressure rise upstream into the isolator section. At $t = 9.8$ seconds the pressure distribution in the combustor was higher than that for the piloted time slice throughout the combustor and nozzle, and an increased pre-combustion pressure rise had fed further forward into the isolator. The pressure distributions shown in Figures 9 and 10 for the piloted and hydrogen only time slices are indicative of robust combustion within the engine. The peak combustor pressure occurred on the cowl-side of the engine for both unfueled and fueled engine operation.

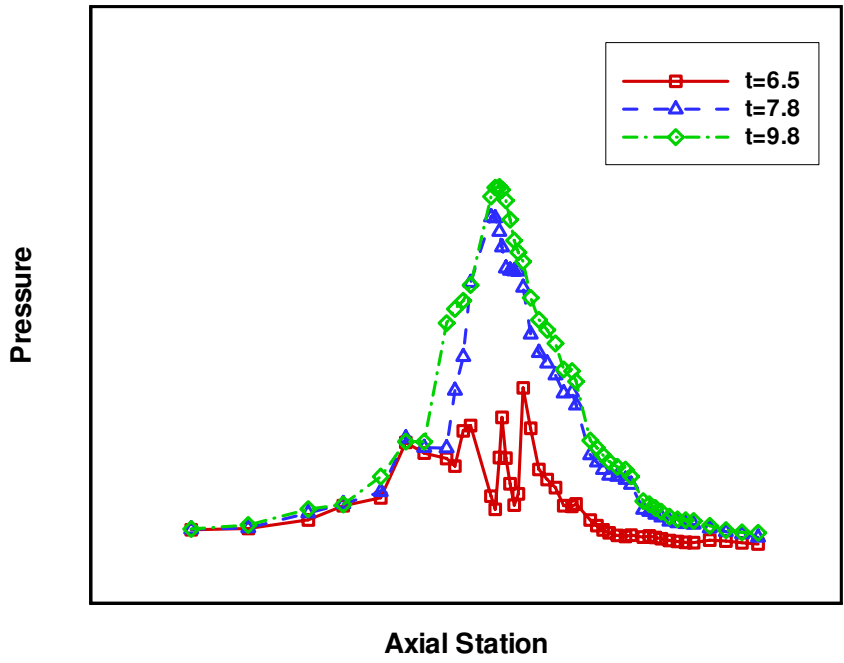


Figure 9. Body-side pressure distributions, typical fueled run.

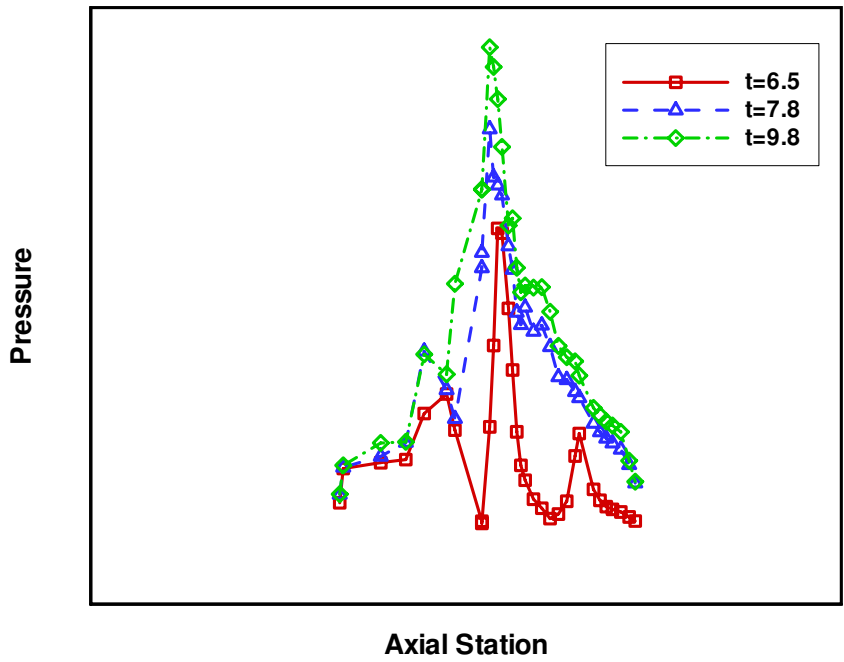


Figure 10. Cowl-side pressure distributions, typical fueled run.

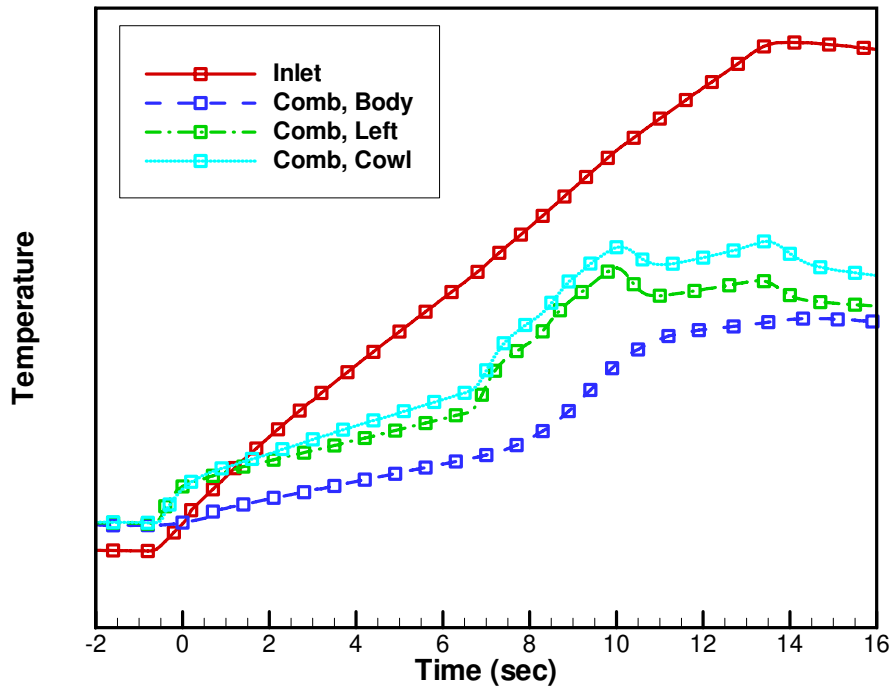


Figure 11. Internal wall temperature measurements.

Co-axial thermocouples measured wall temperatures on the inner and outer walls of the engine. Figure 11 shows the time histories of selected internal wall temperature measurements on the body-side of the inlet upstream of cowl closure, and on the body-side, left-side and cowl-side of the combustor, during this fueled run. All surface temperatures began to rise as facility stagnation conditions were established around $t = -1$ second. The slope of all temperature plots remained relatively constant from $t = -1$ second until approximately $t = 7$ seconds when the silane-hydrogen pilot was established. All combustor temperatures rapidly increased at this time, the change being most obvious on the body and left sides. At approximately $t = 8.0$ seconds the full hydrogen flow was established. This resulted in an increase in the slope of the body-side temperature rise, but had less effect on the other combustor temperatures. Fuel flow to the engine was terminated at approximately $t = 10$ seconds, and the slope of all combustor temperature plots returned approximately to their no-fuel levels, until the vitiated heater was turned off at approximately 13.5 seconds. The temperature on the internal surface of the inlet increased at a constant rate throughout the test, reaching a maximum value significantly higher than that measured on the combustor internal surface, due to the lack of the zirconia coating in the inlet.

V. Conclusions

This paper describes the free-jet testing of a three-dimensional scramjet engine which incorporates an elliptical combustor into an airframe integrated flowpath; and indicates that this REST scramjet performs adequately at simulated Mach 5.3 flight conditions. This REST scramjet had a design point of Mach 7.1 and was intended to operate with fixed geometry between Mach 4.5 and 8.0. The test article included a

truncated forebody plate and was of solid copper construction for heat sink capacity, allowing maximum test durations of 30 seconds.

The flowpath started with the facility at all times at a local approach Mach number of 4.46. Significantly lower stagnation enthalpy fueled tests, which resulted in unstarted engine operation, confirmed the flowpath self-started at this Mach number following termination of the fuel injection. The pressure ratio generated by the inlet was consistent with pre-test CFD predictions. Testing with hydrogen fuel at equivalence ratios between 0.5 and 1.5 indicated that robust combustion was sustained within the engine after the silane-hydrogen pilot was extinguished. Facility-model interactions were experienced for fuel equivalence ratios above 1.1, yet despite this, the flowpath did not unstart at the Mach 5.3 test condition. These results indicate that the inlet/isolator combination utilized in the flowpath is adequate for operation near the lower Mach number range of the design flight regime.

Acknowledgements

This work was supported by the Hypersonic Airbreathing Propulsion Branch and the Creativity & Innovation fund at NASA Langley Research Center, the US Air Force through its Robust Scramjet Program, and Applied Thermal Sciences through SAA1-664. The authors would like to thank Karl Hoose of Applied Thermal Sciences for overall support of the project, Mark Cagle, Tom Hall and the technicians at the Langley machine shop for support during manufacture of the hardware, and NASA technicians Barry Lawhorne, John Simmons, Brian Pierce, Richard Wheeler and Mike Raiford for their support during testing.

References

¹Huebner, L.D., Rock, K.E., Ruf, E.G., Witte, D.W., and Andrews, E.H., "Hyper-X Flight Engine Ground Testing for Flight Risk Reduction", *Journal of Spacecraft and Rockets*, Vol. 38, No. 6, pp 844-852, 2001.

²Smart, M.K., "Design of Three-Dimensional Hypersonic Inlets with Rectangular-to-Elliptical Shape Transition", *Journal of Propulsion and Power*, Vol. 15, No. 3, pp 408-416, 1999.

³Smart, M.K., "Experimental Testing of a Hypersonic Inlet with Rectangular-to-Elliptical Shape Transition", *Journal of Propulsion and Power*, Vol. 17, No. 2, pp 276-283, 2001.

⁴Smart, M.K. and Trexler, C.A., "Mach 4 Performance of a Fixed-Geometry Hypersonic Inlet with Rectangular-to-Elliptical Shape Transition", *Journal of Propulsion and Power*, Vol. 20, No. 2, pp 288-293, 2004.

⁵Smart, M.K., and White, J.A., "Computational Investigation of the Performance and Back-Pressure Limits of a Hypersonic Inlet", *AIAA Paper 2002-0508*, January 2002.

⁶Andrews, E.H, Jr.; Torrence, M.G.; Anderson, G.Y.; Northam, G.B. and Mackley, E.A. "Langley Mach 4 Scramjet Test Facility", TM-862777, 1985.

⁷Rock, K.E., Andrews, E.H. and Eggers, J.M., "Enhanced Capability of the Combustion Heated Scramjet Test Facility", *AIAA Paper 91-2502*, 1991.